

# Characterization of the Solid-Phase Behavior of *n*-Nonylammonium Tetrachlorocuprate by Fourier Transform Infrared Spectroscopy

Guo Ning

Department of Chemistry, Liaoning University, Shenyang 110036, People's Republic of China

Received February 1, 1994; in revised form November 7, 1994; accepted November 9, 1994

The solid-phase behavior of  $[n\text{-C}_9\text{H}_{19}\text{NH}_3]_2\text{CuCl}_4$  was investigated by infrared spectroscopy. The nature of the three solid phases (phase I, phase II, and phase III) is discussed. A temperature-dependent study of infrared spectra provides evidence for the occurrence of structural phase transitions related to the dynamics of the alkyl chains and  $-\text{NH}_3$  polar heads. The phase transition at  $T_{c1}$  (22°C) arises from variation in the interaction and packing structure of the chain. The phase transition at  $T_{c2}$  (34°C) is related to variation in partial conformational order-disorder at the intramolecular level. The GTG or GTG' and small concentration of TG structures near the  $\text{CH}_3$  group are generated in phase III (above 38°C). © 1995 Academic Press, Inc.

## INTRODUCTION

Structural disorder is induced by thermal treatment in many organic systems which contain long alkyl chains. The disorder may be positional, orientational, or conformational. The role played by each type in the disordering process and their detailed nature can be characterized by vibrational spectroscopy(1). In this field, much work has been done both experimentally and theoretically to elucidate the behavior of *n*-alkanes and lipid bilayers in different environments (2).

The bis(*n*-alkylammonium) tetrahalometallates with the general formula  $[n\text{-C}_n\text{H}_{2n+1}\text{NH}_3]_2\text{MX}_4$  ( $M = \text{Cu, Mn, Cd, Zn, Co} \dots$ ;  $X = \text{Cl, Br}$ ) (short notation,  $\text{C}_n\text{M}$ ) belong to this organic system, which undergoes a variety of solid-solid structural phase transitions with high enthalpy. It also presents interesting magnetic and structural properties (3, 4). The potential applications of compounds of this class have drawn the attention of numerous scientists as energy storage materials (5).

These compounds crystallize in a perovskite-type bidimensional layer structure. In the case of  $M = \text{Cu}$  which we studied, the bidimensional macroanions are known to be made up of corner-sharing  $\text{MCl}_6$  octahedra. The general arrangement of the alkyl chain is comparable to the bilayer structure of biological membranes. The

inorganic ion layers are held together by  $\text{N-H} \cdots \text{Cl}$  hydrogen bonds between  $-\text{NH}_3$  polar heads and chlorine atoms.

In this paper, we report temperature-dependent FT-IR spectra of a  $\text{C}_9\text{Cu}$  compound and provide evidence for the occurrence of structural phase transitions related to the dynamics of the alkylammonium ions and  $-\text{NH}_3$  polar heads. The nature of the three solid phases is discussed.

## EXPERIMENTS

### Materials

Bis(*n*-nonylammonium) tetrachlorocuprate was prepared by the reaction of *n*-nonylammonium chloride with stoichiometric amounts of  $\text{CuCl}_2 \cdot 2\text{H}_2\text{O}$  in ethanol. The solvent was evaporated. The solid compound was recrystallized three times from the same solvent and dried under vacuum. The purity of the compound was checked by elemental analysis.

### Spectra

Infrared spectra were recorded on a Perkin-Elmer 1730 Fourier transform infrared spectrometer with KBr pellets. Operating parameters were chosen to provide a resolution of  $1\text{--}2 \text{ cm}^{-1}$  depending on the frequency range. Spectra from 2 to 60°C were obtained with a variable-temperature sample cell built in our laboratory. The accuracy in the temperature measurements is  $\pm 0.5^\circ\text{C}$ .

## RESULTS AND DISCUSSION

Figure 1 shows a DSC curve during heating cycles. There are two transition peaks at  $25.09^\circ\text{C}$  ( $T_{c1}$ ) and  $34.71^\circ\text{C}$  ( $T_{c2}$ ), with transition enthalpies of  $\Delta H_1 = 25.30 \text{ kJ} \cdot \text{mol}^{-1}$  and  $\Delta H_2 = 4.60 \text{ kJ} \cdot \text{mol}^{-1}$ , respectively, corresponding to variations in entropy of  $\Delta S = 99.82 \text{ J} \cdot \text{mol}^{-1} \text{ K}^{-1}$ . The main transition occurs prior to the minor transition.

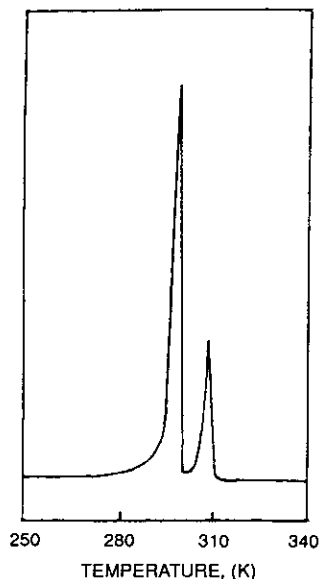


FIG. 1. DSC Curve of a  $C_3Cu$  compound during the heating cycles.

### (1) C-H Stretching Bands

The most important features in the C-H stretching region are the antisymmetric (at  $2920\text{ cm}^{-1}$ ) and symmetric (at  $2850\text{ cm}^{-1}$ )  $CH_2$  stretching modes. Their frequency temperature dependence has been used extensively to monitor order-disorder transitions (6). The increase in wavenumber is partly responsible for the increase in the *gauche* conformation and partly for variation in the density or packing state of the methylene chain (7). The temperature dependence of the wavenumber of the  $CH_2$  symmetric stretching mode is given in Fig. 2. There are three clearly defined regions. The first region (phase I) occurs below  $14^\circ\text{C}$ , the second (phase II) from  $24$  to  $32^\circ\text{C}$ , and the third (phase III) above  $40^\circ\text{C}$ . The first drastic change, centered at  $22^\circ\text{C}$ , marks  $T_{c1}$ , and the second, centered at  $36^\circ\text{C}$ , marks  $T_{c2}$ .

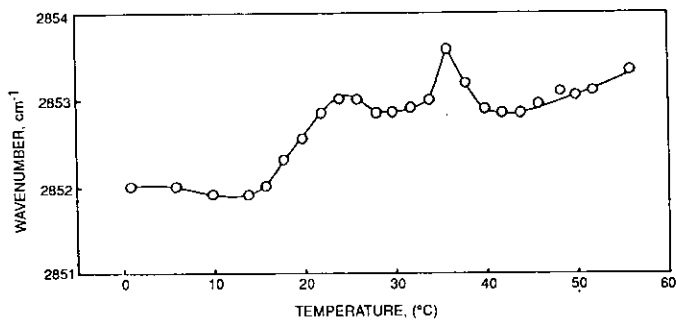


FIG. 2. Temperature dependence of the frequency of the  $CH_2$  symmetric stretching mode.

The change in wavenumber by about  $1\text{ cm}^{-1}$  at  $T_{c1}$  occurs within a  $10^\circ\text{C}$  range and provides evidence of the more flexible nature of the chains. No remarkable change in phase II is observed. Up to  $32^\circ\text{C}$ , the wavenumber begins to increase. It reaches a maximum at  $36^\circ\text{C}$  and then immediately diminishes. This shows that the transition involves only a slight disturbance of the order-disorder structure of the chain near the point of phase transition. The values of the  $\nu_s(CH_2)$  frequency in the spectra of phases II and III are much lower than those found in other systems after melting of long alkyl chains (8). This indicates that a certain degree of conformational order is still present in phases II and III. It is also clearly evident from the spectra in other regions to be discussed below.

### (2) The $1650\text{--}1400\text{ cm}^{-1}$ Region

This region encompasses mainly the bending bands resulting from methylene groups and  $NH_3$  polar heads (in Fig. 3). First, the  $CH_2$  bending band is known to be very sensitive to the intermolecular interaction and is often used as a key band to check the packing state of the methylene chain (9). A  $CH_2$  bending doublet is observed at  $1471$  and  $1466\text{ cm}^{-1}$  at  $6^\circ\text{C}$ . This band-splitting reflects the factor group splitting as a result of interchain interaction in the orthorhombic or monoclinic crystal lattice (10). With increasing temperature, the splitting is reduced. The doublet structure tends to disappear above  $22^\circ\text{C}$  and only a singlet at  $1468\text{ cm}^{-1}$  is observed. On further heating no other noticeable changes are present. The peak wavenumber of these bands is plotted against temperature in Fig. 4. The wavenumber of the band at  $1471\text{ cm}^{-1}$  stays rather constant in phase I. A drastic change of  $3\text{ cm}^{-1}$  corresponding to  $T_{c1}$  occurs between  $20$  and  $24^\circ\text{C}$ . No obvious change in wavenumber above  $24^\circ\text{C}$  is observed. The wavenumber change of the band at  $1466\text{ cm}^{-1}$  occurs about  $10^\circ\text{C}$  below  $T_{c1}$ . The results indicate that rotational motion of the methylene chain as a whole around its axis sets in motion the transition from phase I to phase II.

Figure 4 shows a noncoincidence of transition temperatures between the heating and cooling cycles. The thermal hysteresis of  $10^\circ\text{C}$  suggests that the nonreversibility of the transition temperature is limited to the alkyl chain. The phase transition in all heating and cooling cycles covers a narrow range of  $4^\circ\text{C}$ .

Furthermore, a strong singlet at  $1583\text{ cm}^{-1}$ , assigned to the  $NH_3$  antisymmetric bending mode, and a doublet at  $1491$  and  $1479\text{ cm}^{-1}$ , corresponding to the  $NH_3$  symmetric bending mode in phase I, are observed. The splitting of this mode is due to the crystal field effect. The  $NH_3$  symmetric bending mode in phase II is no longer split, indicating that the  $NH_3$  groups are not locked in a rigid hydrogen-bonded configuration with nonequivalent  $N-H \cdots Cl$

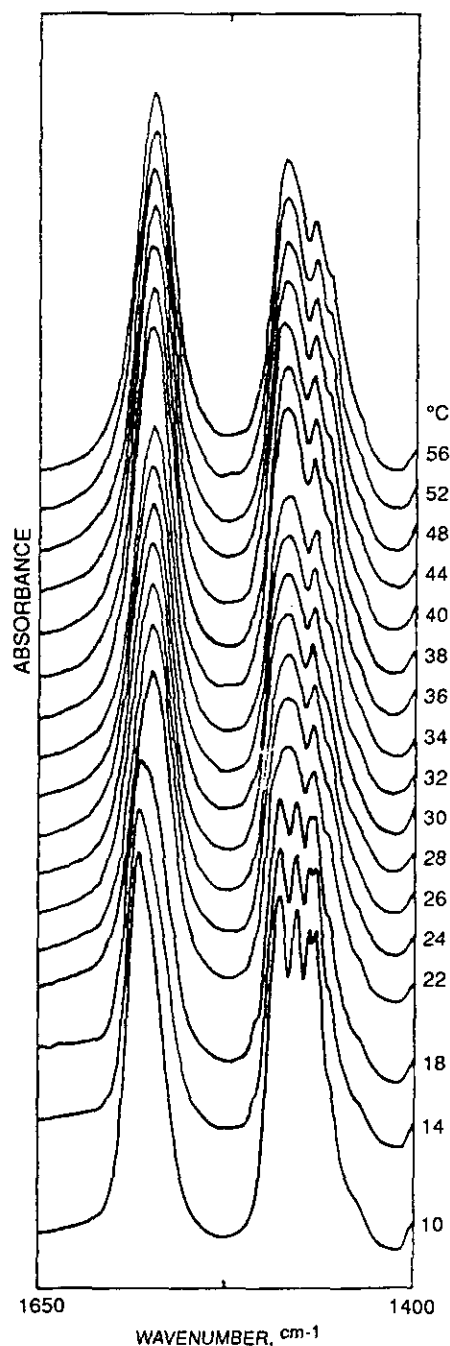


FIG. 3. Temperature dependence of IR spectrum (1650–1400  $\text{cm}^{-1}$ ) of a  $\text{C}_9\text{Cu}$  compound.

bond lengths. The temperature dependence of the wavenumber of  $\delta_{\text{as}}(\text{NH}_3)$  is displayed in Fig. 5. The frequency of  $\delta_{\text{as}}(\text{NH}_3)$  in phase I gradually decreases with increasing temperature and then shifts abruptly to a low value of  $1575 \text{ cm}^{-1}$  between 20 and  $24^\circ\text{C}$ . The frequency above  $24^\circ\text{C}$  remains constant with increasing temperature. These results show that there are an obvious decrease in hydro-

gen bond strength and a change in configuration from phase I to II.

The nonreversible variation of hydrogen bond strength is clearly evident in the plot of cooling cycles. In this case one observes not only thermal hysteresis in the transition temperature, but also noncoincidence of the frequency values between the heating and cooling cycles.

### (3) The Wagging Bands

An important class of spectroscopic signals in this region is due to vibrational modes localized mainly on a few  $\text{CH}_2$  units pinned in specific conformational sequences. These modes are independent of chain length, thus becoming characteristic of specific conformational defects. Their occurrence in the spectrum allows one to probe the existence of geometrical distortion in the alkyl residue.

In the  $1350\text{--}1250 \text{ cm}^{-1}$  region, one can observe the progression of the  $\text{CH}_2$  wagging of the chain (in Fig. 6). The spectra in phase I are characteristic of ordered highly crystalline materials. From phase I to phase II all bands in this region broaden and are accompanied by a reduction of intensity. The valleys between the two wagging bands near  $1320$  and  $1297 \text{ cm}^{-1}$  and between  $1297$  and  $1272 \text{ cm}^{-1}$  are all filled. The bands near  $1306$  and  $1367 \text{ cm}^{-1}$  have been assigned to in-phase and out-of-phase  $\text{CH}_2$  wagging

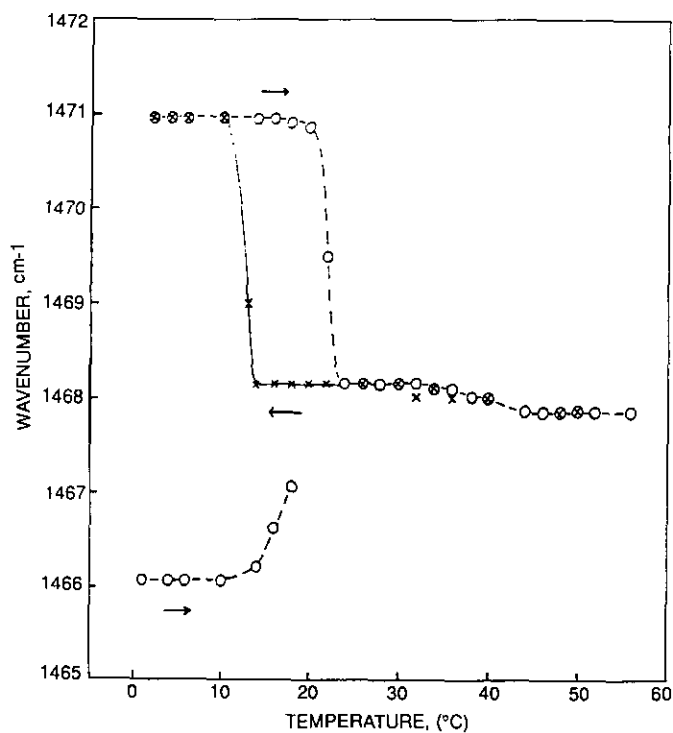


FIG. 4. Temperature dependence of the frequency of the  $\text{CH}_2$  bending mode of a  $\text{C}_9\text{Cu}$  compound.

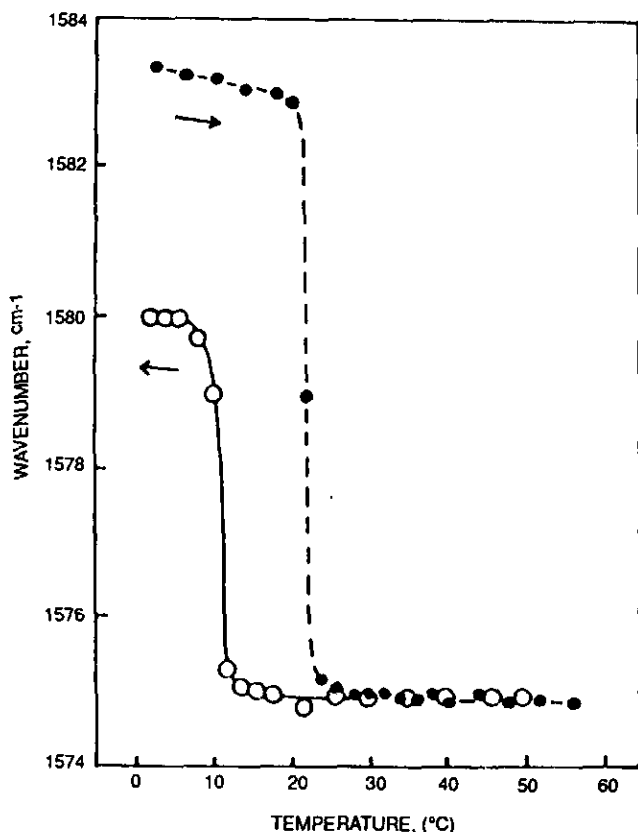


FIG. 5. Temperature dependence of the frequency of the  $\text{NH}_3$  anti-symmetric bending mode of a  $\text{C}_9\text{Cu}$  compound.

motions of the two units in the GTG and GTG' sequences (11, 12). The band at  $1367\text{ cm}^{-1}$  is not observed in phase II. The filling of the valley between  $1320$  and  $1297\text{ cm}^{-1}$  may be due to an enhancement intensity by the mixing of the polar end group  $\text{NH}_3$  and  $\text{CH}_2$  wagging modes with the  $\text{CH}_3$  and  $\text{NH}_3$  internal modes. However, above  $34^\circ\text{C}$ , a clear absorption peak at  $1364\text{ cm}^{-1}$  unquestionably appears and its intensity increases with temperature up to  $56^\circ\text{C}$ .

In phase III, the relative intensity of the band centered near  $1310\text{ cm}^{-1}$  continues to increase while the intensity of the other  $\text{CH}_2$  wagging bands is reduced, except for the band at  $1340\text{ cm}^{-1}$ . From phase I to phase II, the band at  $1337\text{ cm}^{-1}$  shifts abruptly to  $1340\text{ cm}^{-1}$ , it has been assigned mainly to the wagging mode of a single  $\text{CH}_2$  unit in TG conformation near the  $\text{CH}_3$  group (11, 12). Its relative intensity gradually increases with temperature. In phases II and III no evidence of the GG structure is found since the signal at  $1350\text{ cm}^{-1}$ , which has been assigned to the wagging mode of the  $\text{CH}_2$  group isolated between two G structures (11, 12), does not appear.

The results of spectra in this region show that the phase transition at  $T_{c1}$  may arise mainly from variations in the

packing structure of the chain, since no obvious conformational disorder is present. The phase transition at  $T_{c2}$  is related to variations in partial conformational order-disorder at the intramolecular level caused by the presence of GTG or GTG' structures. In phase III, a small concentration of TG structures is generated near the  $\text{CH}_3$  group and the transition occurs in a broad temperature range across the calorimetric transition temperature. A liquid-like state is not reached, however, since the  $\text{CH}_2$  wagging modes are still visible.

#### (4) $\text{CH}_2$ Rocking Bands

As shown in Fig. 7, the spectral evolution of the factor-group doublet for  $\text{CH}_2$  rocking with temperature is similar to that of  $\text{CH}_2$  bending. This doublet is known to result from the effect of the crystal field on the fundamental  $\text{CH}_2$  rocking vibration of the isolated molecules. It is

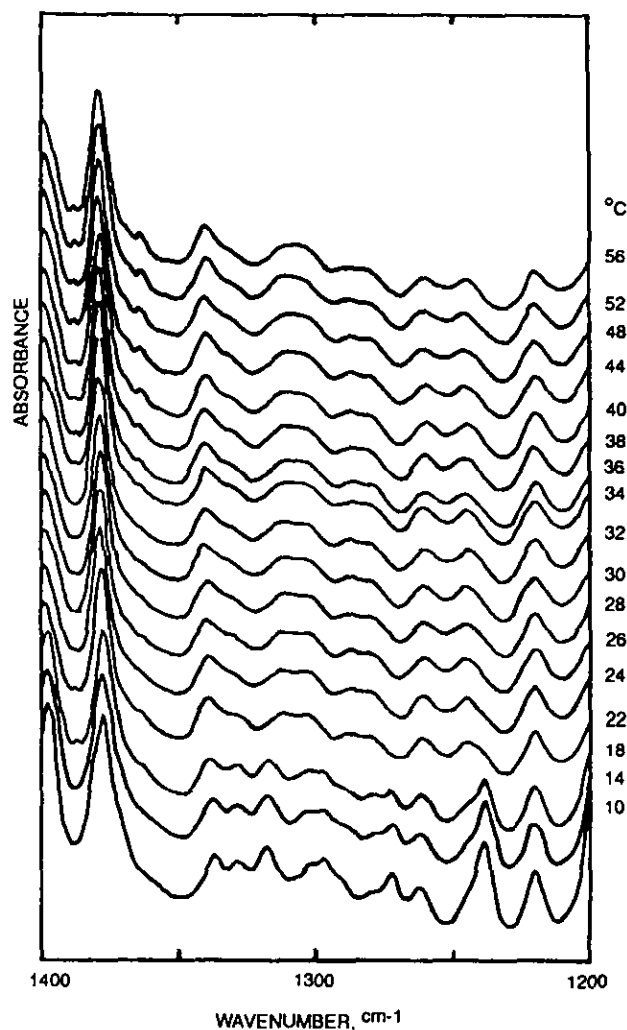


FIG. 6. Temperature dependence of IR spectrum ( $1400\text{--}1200\text{ cm}^{-1}$ ) of a  $\text{C}_9\text{Cu}$  compound.

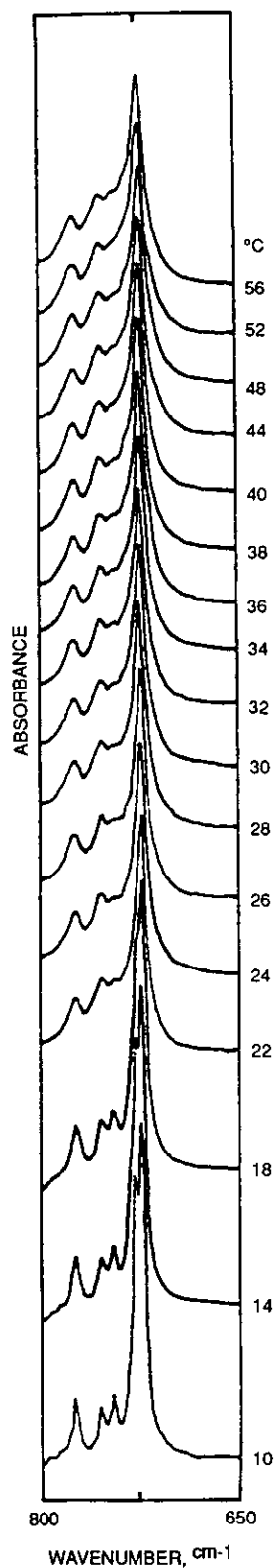


FIG. 7. Temperature dependence of IR spectrum ( $800\text{--}650\text{ cm}^{-1}$ ) of a  $\text{C}_9\text{Cu}$  compound.

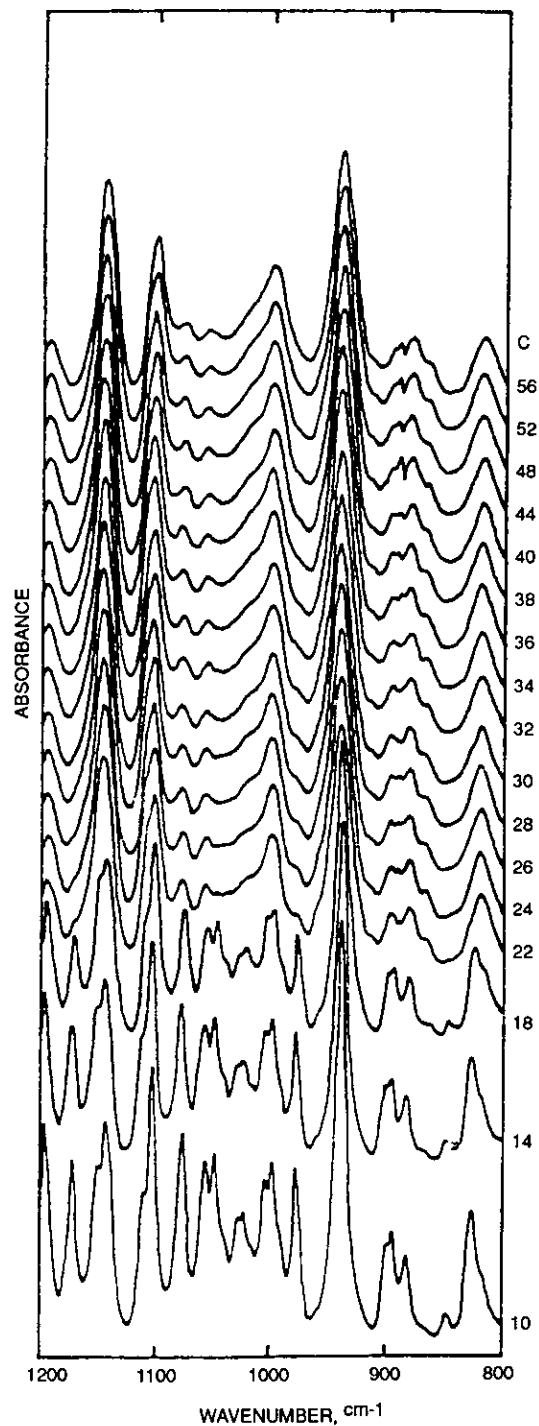


FIG. 8. Temperature dependence of IR spectrum ( $1200\text{--}800\text{ cm}^{-1}$ ) of a  $\text{C}_9\text{Cu}$  compound.

similar to what is generally observed in *n*-alkanes and polyethylenes, the lower wavenumber component being stronger than the other. The doublet in phase I occurs at  $727$  and  $722\text{ cm}^{-1}$ , respectively. When the temperature increases, the splitting is reduced slightly and turns to a

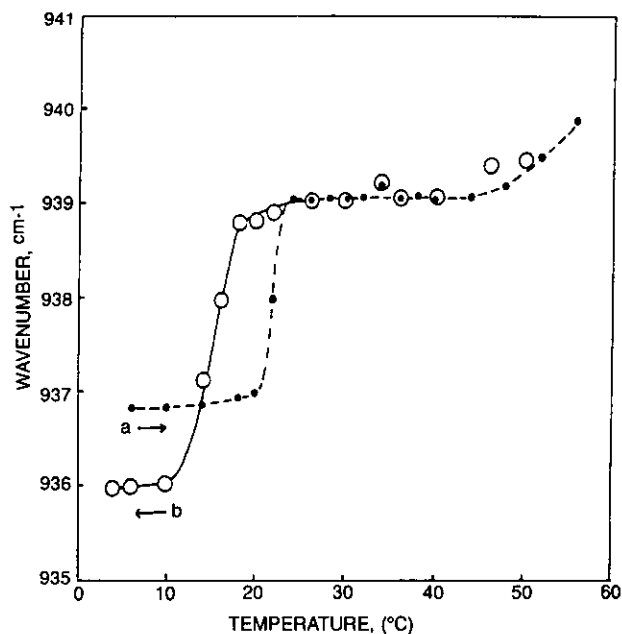


FIG. 9. Temperature dependence of the frequency of the  $\text{NH}_3$  rocking mode: (a) heating, (b) cooling.

singlet above  $22^\circ\text{C}$ . With increasing temperature no other notable changes are observed above  $24^\circ\text{C}$ , except for a slight modification of the band shape (intensity and bandwidth). This result also marks the phase transition at  $T_{c1}$ .

#### (5) The $1200\text{--}800\text{ cm}^{-1}$ Region

This region (in Fig. 8) mainly includes the C–C stretching modes and the  $\text{NH}_3$  rocking modes; the spectrum is very complex. The band at  $1134\text{ cm}^{-1}$  can be assigned to an in-phase stretching mode of all C–C bonds ( $K = 0$ ). The shoulder located at the high-frequency side of the C–C stretching band ( $K = 1$ ) at  $1102\text{ cm}^{-1}$  is more sensitive to the conformation than to the C–C stretching mode ( $K = 0$ ). It shifts to the low wavenumber when the amounts of the *gauche* conformer in the chains increase (13). This shoulder is located near  $1110\text{ cm}^{-1}$  in phase I. With increasing temperature, it shifts gradually toward lower wavenumbers and overlaps with the C–C stretching mode above  $24^\circ\text{C}$ .

The intense band at  $937\text{ cm}^{-1}$  arises mainly from the rocking mode of N–H bonds, except for the overlap with the C–C stretching band. Its frequency temperature dependence is shown in Fig. 9. The change of  $2\text{ cm}^{-1}$  centered at  $22^\circ\text{C}$  marks the phase transition at  $T_{c1}$ , indicating a rearrangement of the  $\text{NH}_3$  polar heads in such a way

that the hydrogen bonds have the same lengths. There is no obvious change near  $T_{c2}$ . This is similar to the  $\text{NH}_3$  antisymmetric bending mode and also shows thermal hysteresis of about  $10^\circ\text{C}$  on cooling cycles and noncoincidence of the frequency values between the heating and cooling cycles. It was also found that the bands appearing at  $977$ ,  $1027$ ,  $1056$ ,  $1075$ , and  $1173\text{ cm}^{-1}$  are sensitive to the packing structure of the chain. The intensity is rapidly reduced at  $T_{c1}$ , and some bands even disappear.

## CONCLUSION

From the above studies of the spectra, we can conclude that (1) the main phase transition at  $T_{c1}$  results from variation in the interaction and packing structure of the chain and is accompanied by rearrangement of the configuration bond and by an obvious decrease in strength of hydrogen bonds. A certain degree of conformational order is still present in phase II. (2) The phase transition at  $T_{c2}$  is related to the variation in the partial conformational order–disorder owing to the occurrence of the GTG or GTG' and the TG structures near  $\text{CH}_3$  groups. Phase III does not reach a liquid-like state. (3) The motions of the  $\text{NH}_3$  polar heads and the chains are all subject to thermal hysteresis.

## REFERENCES

1. Guo Ning, Zeng Guangfu, and Xi Shiquan, *J. Phys. Chem. Solids* **53** (3), 437 (1992).
2. R. Mendelsohn, G. Anderle, M. Jaworsky, H. H. Mantsch, and R. A. Dluhy, *Biochim. Biophys. Acta* **775**, 215 (1984).
3. M. R. Ciajolo, P. Cooradini, and V. Pavone, *Gazz. Chim. Ital.* **B106**, 807 (1976).
4. R. Blinc, M. Burgar, B. Lozar, J. Seliger, J. Slak, and V. Butar, *J. Chem. Phys.* **66**, 278 (1977).
5. V. Busico, C. Carfagna, V. Salerno, M. Vacatello, and F. Fittipaldi, *Solar Energy* **124**, 575 (1980).
6. H. L. Casal, D. G. Cameron, and H. H. Mantsch, *J. Phys. Chem.* **89**, 5557 (1985).
7. D. G. Cameron, J. Umemura, P. T. T. Wong, and H. H. Mantsch, *Colloids Surf.* **4**, 131 (1982).
8. H. H. Mantsch, A. Martin, and D. G. Cameron, *Biochemistry* **20**, 3138 (1981).
9. D. G. Cameron, H. L. Casal, E. F. Gudgin, and H. H. Mantsch, *Biochim. Biophys. Acta* **596**, 463 (1980).
10. H. L. Casal, H. H. Mantsch, and D. G. Cameron, *Solid State Commun.* **49**, 573 (1984).
11. L. Ricard, R. Cavagnat, and M. Rey-Lfon, *J. Phys. Chem.* **89**, 4887 (1985).
12. L. Ricard, M. Rey-Lafon, and C. Biran, *J. Phys. Chem.* **88**, 5614 (1984).
13. R. G. Snyder, *J. Chem. Phys.* **47**, 1316 (1967).